Cell, Vol. 102, 43–53, July 7, 2000, Copyright ©2000 by Cell Press

Identification of DIABLO, a Mammalian Protein that Promotes Apoptosis by Binding to and Antagonizing IAP Proteins

Anne M. Verhagen,* Paul G. Ekert,*‡ Miha Pakusch,* John Silke,* Lisa M. Connolly,† Gavin E. Reid,† Robert L. Moritz,† Richard J. Simpson,† and David L. Vaux*§

*The Walter and Eliza Hall Institute of Medical Research
Post Office Royal Melbourne Hospital
Victoria 3050
†Joint Protein Structure Laboratory
Ludwig Institute for Cancer Research and
The Walter and Eliza Hall Institute of Medical Research
Post Office Box 2008
Royal Melbourne Hospital
Victoria 3050
‡The Murdoch Children's Research Institute
Royal Children's Hospital
Flemington Road, Parkville
Victoria 3052
Australia

Summary

To identify proteins that bind mammalian IAP homolog A (MIHA, also known as XIAP), we used coimmunoprecipitation and 2D immobilized pH gradient/SDS PAGE, followed by electrospray ionization tandem mass spectrometry. DIABLO (direct IAP binding protein with low pI) is a novel protein that can bind MIHA and can also interact with MIHB and MIHC and the baculoviral IAP, OpIAP. The N-terminally processed, IAP-interacting form of DIABLO is concentrated in membrane fractions in healthy cells but released into the MIHA-containing cytosolic fractions upon UV irradiation. As transfection of cells with DIABLO was able to counter the protection afforded by MIHA against UV irradiation, DIABLO may promote apoptosis by binding to IAPs and preventing them from inhibiting caspases.

Introduction

Apoptosis is a highly conserved process by which metazoan organisms remove unwanted cells (Vaux and Korsmeyer, 1999). The key effector enzymes of apoptosis are a family of cysteine proteases termed caspases (Alnemri et al., 1996). Upstream caspases are activated by adaptor proteins such as FADD and Apaf-1, which bind to the prodomains of the caspase zymogens (Boldin et al., 1996; Muzio et al., 1996; Zou et al., 1997). The ability of the adaptor molecules to activate the caspases can be controlled by several families of regulatory molecules. For example, apoptosis signaled via Apaf-1 can be inhibited by antiapoptotic members of the Bcl-2 family (Hu et al., 1998; Pan et al., 1998; Moriishi et al., 1999), and apoptosis signaled by FADD can be inhibited by FLIP (Irmler et al., 1997).

Experiments in insect and mammalian systems have shown that caspase-dependent apoptosis can also be regulated by members of the inhibitor of apoptosis (IAP) protein family. IAPs were first identified as baculoviral gene products that inhibited the defensive apoptotic response of insect cells following infection (Crook et al., 1993). Subsequently, IAP homologs have been identified in both invertebrates and vertebrates (Rothe et al., 1995; Duckett et al., 1996; Liston et al., 1996; Uren et al., 1996).

DIAP1 from *Drosophila melanogaster* can bind to and inhibit *Drosophila* caspases DCP-1, DRICE, and DRONC (Kaiser et al., 1998; Dorstyn et al., 1999; Hawkins et al., 1999). Inhibition of apoptosis by DIAP1 can be countered by insect proapoptotic signaling molecules Grim, Reaper, and HID, which appear to promote caspase activation by binding directly to DIAP1 and thereby preventing it from inhibiting caspase activity (Hay et al., 1995; Kaiser et al., 1998; Wang et al., 1999). While no mammalian homologs of Grim, Reaper, or HID have been identified, because baculoviral and insect IAPs are able to inhibit apoptosis in mammalian cells, their mechanism of action is likely to be conserved (Hay et al., 1995; Hawkins et al., 1996).

The mammalian IAP homolog A (MIHA, XIAP, h-ILP) inhibits apoptosis induced by chemotherapeutic drugs or UV radiation and expression of Bax or caspases (Duckett et al., 1996; Liston et al., 1996; Uren et al., 1996; Deveraux et al., 1998) and is able to directly bind to caspases-3 and -7 and pro-caspase-9 (Deveraux et al., 1997, 1998). We hypothesized that, like insect IAPs, mammalian IAPs may be regulated by proapoptotic signaling molecules that bind to them and stop them from inhibiting caspase activity.

In order to find such molecules, we transiently transfected 293T cells with epitope-tagged mouse MIHA and coimmunoprecipitated associated proteins. We separated these proteins by 2D immobilized pH gradient (IPG)/SDS PAGE and sequenced them by electrospray ionization tandem mass spectrometry. Here, we report the identification of DIABLO, a proapoptotic protein that can directly interact with mammalian and baculoviral IAPs and interfere with MIHA-mediated UV protection presumably by dislodging active IAP bound caspases.

Results

Identification of DIABLO

293T cells were transiently transfected with a cDNA encoding MIHA with a carboxy-terminal Flag epitope tag (Flag-MIHA) or a cDNA encoding control Flag-tagged CrmADQMD variant (Flag-DQMD, Ekert et al., 1999). Flag-MIHA and Flag-DQMD were immunoprecipitated from ^{35}S-labeled cell lysates with anti-Flag mAb-coupled agarose beads and the immunoprecipitate examined by 2D IPG/SDS PAGE. Four proteins were observed

§To whom correspondence should be addressed (e-mail: vaux@wehi.edu.au).

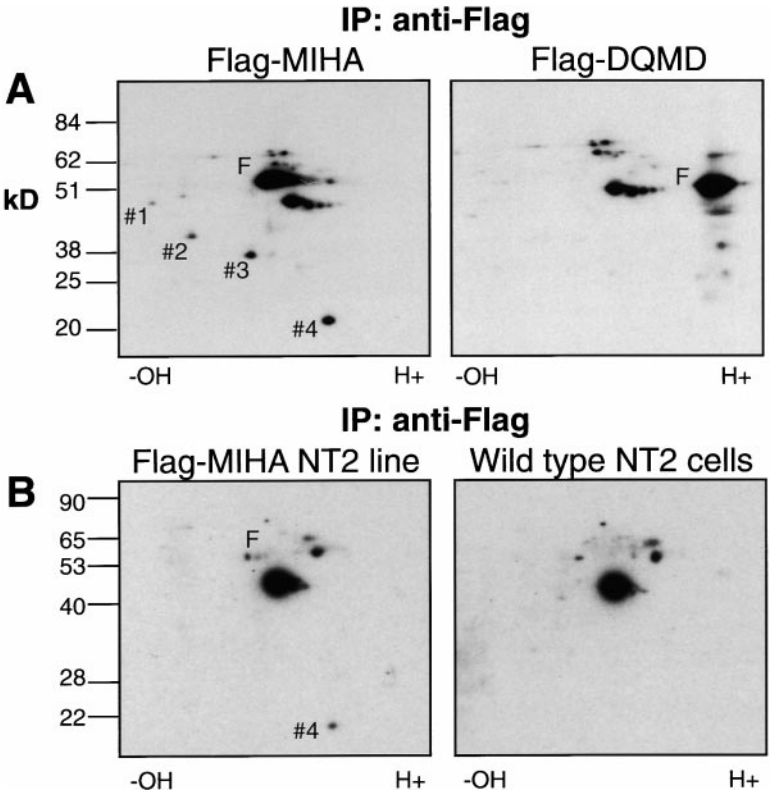

Figure 1. Detection of MIHA Interacting Proteins

(A) Flag-MIHA (C-term) and Flag-DQMD (N-term) were immunoprecipitated from ^{35}S-labeled lysates of transiently transfected 293T cells using Flag-specific mAb M2 coupled agarose beads. The immunoprecipitate was analyzed by IPG/SDS PAGE, and proteins visualized by autoradiography. Four proteins, #1 to #4, were detected that specifically immunoprecipitate with Flag-MIHA but not the control protein Flag-DQMD. Flag-tagged proteins are indicated by "F."

(B) Immunoprecipitates prepared from ^{35}S-labeled lysates of control NT2 cells and an NT2 cell line stably expressing Flag-MIHA (N-term) were examined by IPG/SDS PAGE for MIHA interacting proteins. Flag-MIHA migrated as a series of small spots and is indicated by the "F." Coimmunoprecipitated protein spot #4 is clearly visible.

coimmunoprecipitating with Flag-MIHA that were not observed in immunoprecipitates of the control Flag-tagged protein (Figure 1). These four proteins also coimmunoprecipitated with MIHA bearing an amino-terminal Flag epitope tag transfected into 293T cells (data not shown). Furthermore, when experiments were carried out in neuronal NT2 cells stably expressing low levels of N-terminally Flag-tagged MIHA, although three of the proteins could no longer be immunoprecipitated, one, #4, a 23 kDa protein with a low pI of approximately 5.3, was still able to interact. This suggested that the binding between MIHA and protein #4 was physiological and unlikely to be a consequence of overexpression.

Cloning of DIABLO

In order to identify protein #4, cellular lysates prepared from 100 × 15 cm petri dishes of 293T cells transiently transfected with Flag-MIHA were passed through a column of anti-Flag antibody-coupled agarose beads. After extensive washing, the bound proteins were eluted with acidic glycine and separated by 2D IPG/SDS PAGE (Figure 2A). A Coomassie stained gel spot corresponding to protein #4 was digested in situ with trypsin. The resultant peptides were extracted from the gel, subsequently resolved by capillary column RP-HPLC, and sequenced by electrospray-ionization tandem mass spectrometry (Figures 2B–2E). Since automated database searching of the uninterpreted MS/MS spectra to identify the peptides was unsuccessful, manual de novo sequence analysis was employed to obtain either partial or complete amino acid sequence information on six peptides.

The peptide sequences recovered were used to search DNA EST databases using TFASTA and TBLASTN. Perfect agreement was found with both human and mouse sequences. The murine IMAGE consortium EST clone (accession number AA276162) that extended most 5′ was obtained from Research Genetics and fully sequenced. This 1356 bp cDNA clone extended further 5′ than the human ESTs available and had an open reading frame encoding a 237 amino acid protein with predicted molecular weight of 26.8 kDa and pI of 6.5. This is slightly larger and more basic than that of the isolated protein #4, suggesting posttranslational modification. Although no upstream stop codon was present, two rat EST clones (AA686702 and H35263) commencing at approximately the same site and with the same open reading frame were noted in the database. Further searches of the DNA databases using the full-length mouse sequence also revealed a homolog in the Japanese flounder (EST1197472). No peptide motifs could be recognized using the PROSITE database. However, the human DIABLO sequences are identical to those of Smac, independently identified by Du et al. (2000).

DIABLO Expression Pattern

Northern analysis of mRNA from adult mouse tissues showed that a 1.4 kb DIABLO message was most abundant in heart, liver, kidney, and testis. Expression was not readily detected in skeletal muscle, lung, spleen, or brain (Figure 3). Nevertheless, human DIABLO ESTs derived from lung and cerebellum were noted in the database along with ESTs from kidney, heart, uterus, and placenta.

MIHA Interacts with DIABLO

To confirm that the cDNA obtained corresponded to MIHA interacting protein #4, we transfected 293T cells

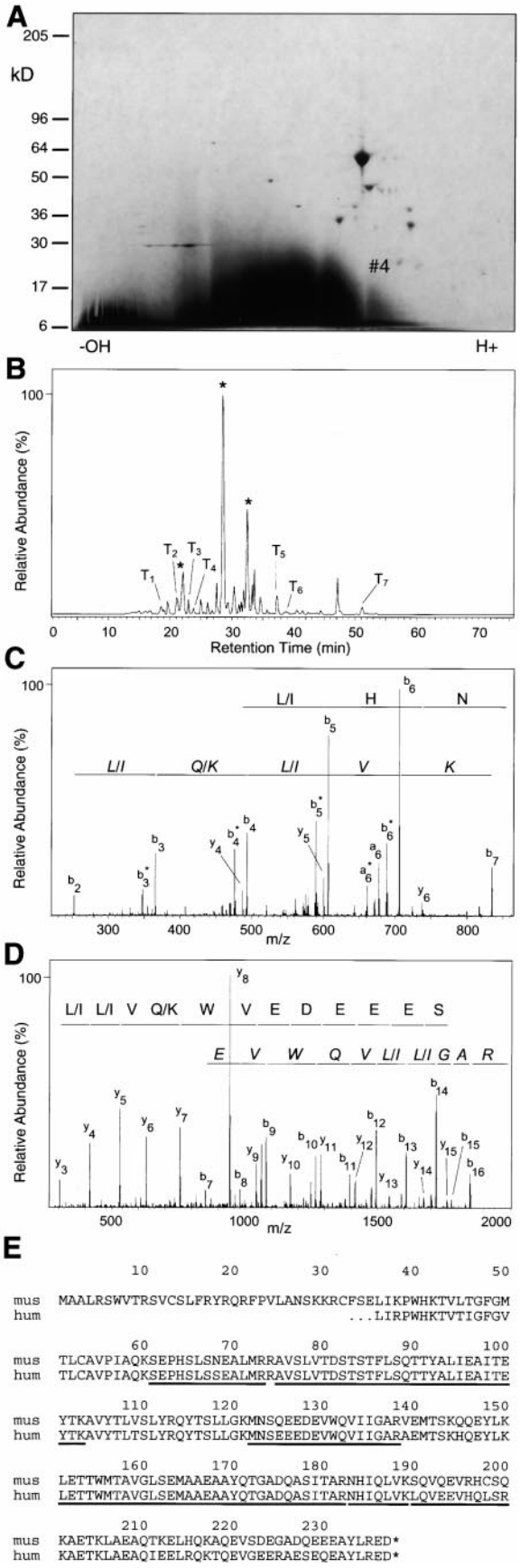

with cDNA encoding Flag-MIHA together with cDNA encoding putative murine protein (DIABLO) tagged on its carboxy terminus with a HA epitope (HA-DIABLO). Immunoprecipitations were prepared from ^{35}S methionine-labeled cell extracts using either anti-Flag coupled agarose beads or anti-HA antibody plus protein G sepharose and were analyzed by 2D IPG/SDS PAGE (Figures 4A and 4B). In the anti-HA immunoprecipitations, DIABLO was present in two forms, a 29 kDa protein with a pI of approximately 6.1 and a 24 kDa protein with a pI of approximately 5.4 (Figure 4A). It is likely that the smaller protein represented a processed form of DIABLO

Figure 2. Identification of DIABLO

(A) Flag-MIHA was purified from transiently transfected 293T cells and with associated proteins was separated by 2D IPG/SDS PAGE and visualized with Coomassie blue. Protein #4 (DIABLO) was extracted from the gel for peptide analysis.

(B) Capillary column RP-HPLC/ESI-MS/MS of a tryptic digest of DIABLO. The unfractionated peptide mixture (30 μL, ~0.2 pmol from a total volume of ~100 μl) was applied to the 0.2 mm ID column at 6 μl/min. The column was developed at 1.6 μl/min using a linear 60-min gradient from 0%–100% B, where solvent A was 0.1% aqueous trifluoroacetic acid and solvent B was 60% acetonitrile in 0.1% aqueous trifluoroacetic acid. Peptides were sequenced by collision-induced dissociation (CID) of their $[M+H]^+$ and $[M+2H]2^+$ ions. Peaks labeled with an asterisk were identified as trypsin autodigestion peptides.

(C) Collision-induced dissociation—MS/MS spectrum of the singly-charged ion of tryptic peptide T1 (*m/z* 851.8). The amino acid sequence NH(L/I)(Q/K)(L/I)VK was determined by interpretation of the b- (italic text) and y-type (normal text) product ion series as shown (since the residues L/I are isobaric and K/Q have the same nominal mass, these amino acid residue pairs were not able to be differentiated using the instrumentation employed in this study).

(D) Collision-induced dissociation MS/MS spectrum of the doubly-charged ion of tryptic peptide T5 (*m/z* 1011.6). The amino acid sequence XXSEEEDEVW(Q/K)V(L/I)(L/I)GAR was determined by manual de novo interpretation of the b- (italic text) and y-type (normal text) product ion series (Roepstorff and Fohlman, 1984) as shown. (X = unknown amino acid; since the residues L/I are isobaric and K/Q have the same nominal mass, these amino acid residue pairs were not able to be differentiated using the instrumentation employed in this study). Following identification of the cDNA, the unidentified residues XX were shown to correspond to MetAsn. The difference in observed (2021.6 D) versus calculated (2005.2 D) mass suggests that the methionine was present as the sulfoxide. Using the same approach, the following partial sequences were obtained for T2-T4 and T6-T7: T2 (obs. mass 1459.6 D...PHS(L/I)...A(L/I)M (so)R) note that M(so) corresponds to methionine sulfoxide; T3 (obs. mass 1339.3 D ((Q/K)(L/I))VEEVH(Q/K)(L/I)SR) Note that the order of the two N-terminal amino acids was not able to be determined; T4, (obs. mass 1444.1 D...PHS(L/I)S...); T6 (obs. mass 3376.4 D ...AAEAAY(Q/K)TGAD(Q/K)A...); T7 (obs. mass 3153.9 D...(L/I)S (Q/K)TTYA(L/I)(L/I)EA(L/I)...). Inspection of the identified protein sequence determined the complete sequences of peptides T1-T7 as: T1, NHIQLVK, calc. mass 851.0; T2, SEPHSLSSEALM(so)R calc. mass 1459.6; T3, LQVEEVHQLSR calc. mass 1337.5; T4, SEPHSLS SEALMR calc. mass 1443.6; T5, M(so)NSEEEDEVWQVIIGAR calc. mass 2021.2; T6, LETTWM(so)TAVGLSEM(so)AAEAAYQTGADQASI TAR calc mass 3377.7; T7, AVSLVTDSTSTFLSQTTYALIEAITEYTK calc. mass 3154.5.

(E) Comparison of mouse and human DIABLO. The human sequences shown correspond to DNA sequences AA3038, T53449, T53449, AA3257, and AA1299. Human DIABLO peptide sequences identified by mass spectroscopic sequencing are underlined. Cleavage of the N-terminal fragment must occur upstream of the first peptide, i.e., at residue 60 or before. The human DIABLO sequences are identical to those of Smac, independently identified by Du et al. (2000).

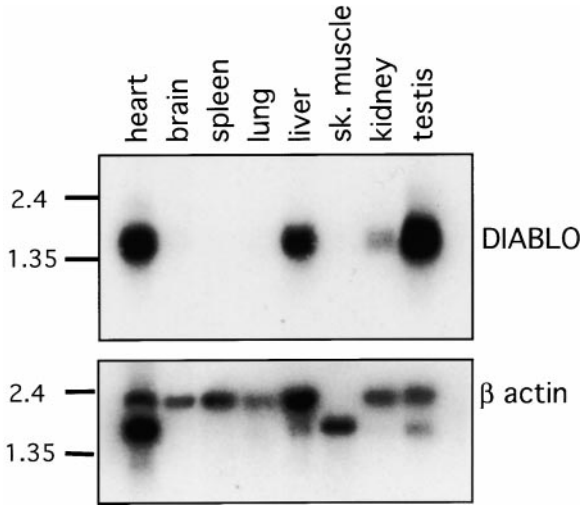

Figure 3. Expression of DIABLO in Adult Mouse Tissues

Northern blots of polyA mRNA were hybridized with a probe encompassing the entire coding region of DIABLO. The blot was stripped and rehybridized with a β-actin probe.

from which the N terminus had been cleaved. A protein with slightly lower molecular weight and slightly higher pI than the smaller of the HA-tagged spots was also be detected. This protein had the same mobility pattern as endogenous human protein spot #4 and was not recognized by anti-HA antibodies in Western analysis (data not shown) and was therefore likely to be endogenous DIABLO. Because anti-HA antibodies were able to coimmunoprecipitate endogenous DIABLO along with transfected HA-tagged DIABLO, two or more DIABLO molecules must be able to form complexes in either the presence or absence of MIHA.

Flag-MIHA was clearly detected in the anti-HA immunoprecipitations from cells cotransfected with cDNAs encoding HA-tagged DIABLO and Flag-MIHA, whereas an unrelated Flag-tagged protein, Flag-DQMD, did not coimmunoprecipitate with HA-DIABLO. In addition, Flag-MIHA did not coimmunoprecipitate with an unrelated HA-tagged control. The high levels of ^{35}S-labeled Flag-MIHA present in the immunoprecipitates of HA-DIABLO strongly suggest that there is a direct interaction between DIABLO and MIHA.

In immunoprecipitates of Flag-MIHA from cells transfected with Flag-MIHA alone, endogenous DIABLO is indicated (Figure 4B). In Flag-MIHA immunoprecipitates from cells cotransfected with cDNA encoding untagged murine DIABLO, a much stronger signal at this exact location was seen, presumably representing the coexpressed untagged murine DIABLO protein. In MIHA immunoprecipitates from cells cotransfected with MIHA and HA-tagged DIABLO, a protein was detected that migrated slightly above and with a more acidic pI than the endogenous molecule that was also visible. This slight shift in molecular weight and increased acidity can be accounted for by the HA tag. Interestingly, although DIABLO is present in the anti-HA immunoprecipitates in two forms, MIHA interacts preferentially with the lower molecular weight, low pI, processed form.

The specificity of the DIABLO-MIHA interaction was also demonstrated by Western blot analysis. Flag-MIHA specifically coimmunoprecipitated HA-DIABLO but not two unrelated HA-tagged proteins HA-FLN29 and HA-ZAP1 (Figure 4C). HA-DIABLO was not coimmunoprecipitated with Flag-DQMD. In reverse, HA-DIABLO specifically coimmunoprecipitated Flag-MIHA but not Flag-DQMD, and Flag-MIHA was not coimmunoprecipitated with control HA-FLN29 (Figure 4D).

DIABLO Interacts with Several Antiapoptotic IAPs

To test whether DIABLO is able to interact with other IAPs, we transfected 293T cells with cDNAs encoding Flag-tagged IAPs together with HA-DIABLO. The IAPs were immunoprecipitated with anti-Flag mAb-coupled agarose beads and the immunoprecipitates examined for the presence of DIABLO by Western analysis using anti-HA antibodies (Figure 5). As before, DIABLO was present in the whole cell lysate (WCL) in two forms, but MIHA interacted preferentially with the processed form, with only weak interaction with the nonprocessed protein being detectable. MIHB, MIHC, and the baculoviral IAP from *Orgyia pseudotsugata* NPV, OpIAP, but not the control Flag-DQMD, were also able to interact with the processed form of DIABLO. Although less HA-DIABLO was detectable in these immunoprecipitates, these proteins were not very highly expressed in 293T cells. This was evident when the membrane was probed with anti-Flag mAb, where the signal for OpIAP was very weak compared to that of Flag-MIHA and Flag-DQMD, and Flag-MIHB and Flag-MIHC were not detectable. Flag-MIHB and Flag-MIHC could be detected following sequential probing of the membrane with the more sensitive cIAP1- and cIAP2-specific mAbs, respectively. These results indicate that despite low expression of MIHB and MIHC, there is a high stoichiometry of interaction between these IAPs and DIABLO.

Subcellular Localization of DIABLO

To confirm whether the interaction between IAPs and DIABLO could occur in vivo, we examined whether they reside in the same cellular compartment. 293T cells transiently expressing Flag-MIHA and HA-DIABLO were harvested and lysed in hypotonic buffer by passaging through a 27G needle (see Experimental Procedures). The extracts were then separated by centrifugation on 50%–10% sucrose gradients and the fractions analyzed by Western blot using a series of antibodies (Figure 6A).

Membrane-associated proteins localized to the high-percentage sucrose fractions, i.e., the bottom three to four fractions collected, as indicated by the presence of the mitochondrial membrane protein VDAC and the ER-associated protein calnexin. Although small amounts of cytochrome c, a non-membrane-associated mitochondrial protein, were also evident in these compartments, it was much more abundant in the cytosolic fractions, presumably due to mitochondrial leakage during extraction. Flag-MIHA was in the more buoyant cytosolic fractions and was virtually absent in membrane fractions, as was caspase-3. Interestingly, although the larger form of DIABLO was in the membrane-associated fractions, N-terminally processed DIABLO, the form that preferentially interacts with MIHA, colocalized with

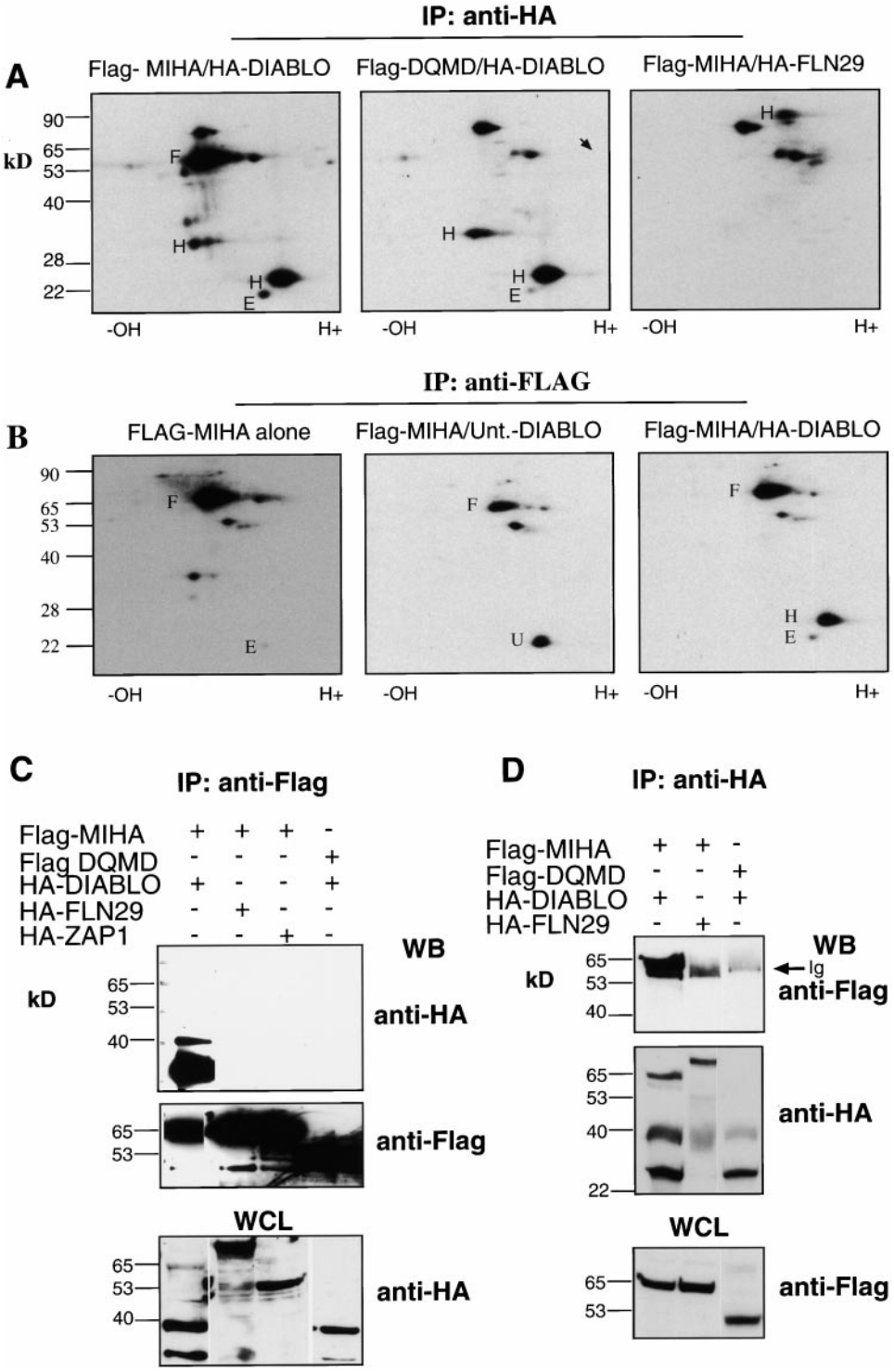

Figure 4. Specific Interaction of MIHA with DIABLO

Anti-HA (A) and anti-Flag (B) immunoprecipitates prepared from ^{35}S-labeled lysates of transiently transfected 293T cells were analyzed by IPG/SDS PAGE. Flag-tagged proteins are denoted by "F", HA-tagged proteins by "H", endogenous DIABLO by "E," and untagged transfected DIABLO (unt. DIABLO) by "U". An arrow indicates where the negative control protein Flag-DQMD would normally migrate. (C) Flag-MIHA (C-term) and Flag-DQMD were immunoprecipitated from transiently transfected 293T cells and interaction with cotransfected molecules HA-DIABLO and control HA-tagged proteins FLN29 and ZAP1 examined by Western blot analysis with anti-HA antibody. Directly immunoprecipitated Flag-tagged proteins were subsequently demonstrated by reprobing the membrane with anti-Flag mAb and expression of the HA-tagged proteins confirmed by anti-HA western blot analysis of whole cell lysate (WCL). (D) Immunoprecipitates of HA-DIABLO and control protein HA-FLN29 from transiently transfected 293 T cells were examined for coimmunoprecipitating FLAG-MIHA or FLAG-DQMD by Western blot analysis with anti-Flag antibody as indicated. Flag-MIHA can be seen in the HA-DIABLO immunoprecipitate migrating just above the Ig band. The directly immunoprecipitated HA-tagged proteins were subsequently demonstrated by reprobing of the membrane with anti-HA antibody. Some residual Flag-MIHA signal is present in lane 1 from the previous blot. Expression of the Flag-tagged proteins was confirmed by anti-Flag Western blot analysis of WCL.

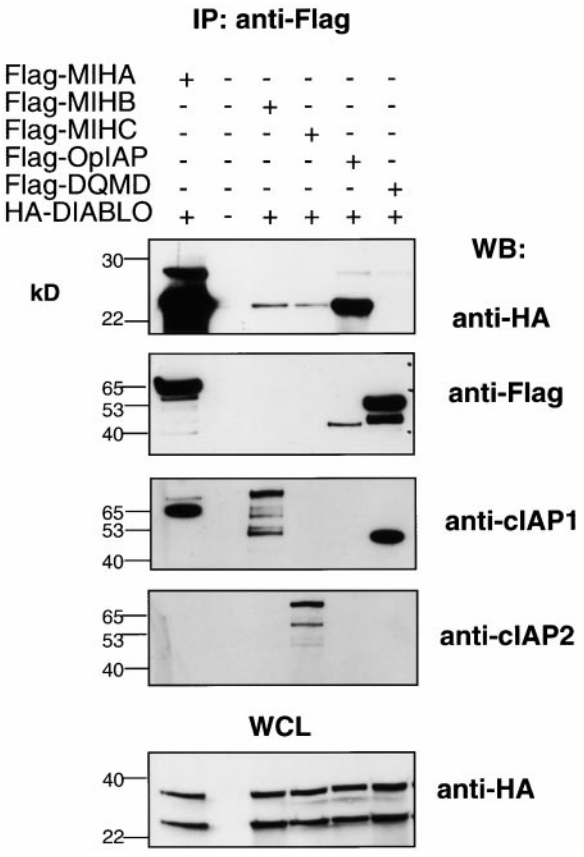

Figure 5. Interaction of DIABLO with Mammalian IAPs MIHA, MIHB, MIHC, and OpIAP

Flag-epitope-tagged IAPs and control Flag-DQMD were immunoprecipitated from transiently transfected 293T cells and the immunoprecipitates examined for cotransfected HA-DIABLO by anti-HA Western blot analysis. The directly immunoprecipitated proteins were then demonstrated by sequential probing of the membrane with anti-Flag, anti-cIAP1, and anti-cIAP2 antibodies. The signals in lanes 1 and 6 of the anti-cIAP1 Western blot represent residual anti-Flag signals from Flag-MIHA and Flag-DQMD, respectively. Expression of HA-DIABLO was confirmed by anti-HA Western of WCL.

MIHA in the cytosol, in addition to being present in the membrane fractions.

The presence of DIABLO in the cytosolic fractions of transiently transfected 293T cells may have been due to overexpression and/or cellular toxicity resulting from the transfection procedure. To determine the localization of endogenous DIABLO, we used a polyclonal antibody kindly provided by Dr. Xiaodong Wang (Du et al., 2000) to detect DIABLO in the neuronal cell line NT2 before and after UV irradiation (Figure 6B). Although the unprocessed form of DIABLO was detectable when it was overexpressed in 293T cells (Figure 6A) or NT2 cells (data not shown), only the processed form of endogenous DIABLO was apparent. Mature DIABLO was found in the membrane fractions in healthy cells with minimal amounts in the cytosolic fractions. Upon exposure of the cells to UV radiation, the amount of DIABLO in the membrane fractions decreased, and DIABLO appeared in the cytosolic fractions. Simultaneously, the amount of cytochrome c was reduced in the membrane fractions and increased in the cytosolic fractions (Figure 6B). The results shown are from NT2 cells stably transfected with Flag-MIHA that are resistant to UV-induced apoptosis (Figure 7). Similar subcellular translocation of endogenous DIABLO was observed in wild-type cells following UV treatment (data not shown). These results demonstrate that although DIABLO is normally localized in membrane compartments within the cell, it is released upon UV treatment into the cytosol where it can interact with IAPs. Importantly, MIHA does not prevent release of either DIABLO or cytochrome c from their membrane association.

As described by Du et al. (2000), DIABLO has at its N terminus a stretch of amino acids characteristic of mitochondrial targeting sequences that are normally removed from proteins upon import into mitochondria. To examine whether this sequence was sufficient for targeting DIABLO to the mitochondria, we prepared a construct encoding a protein possessing the N-terminal 53 amino acids of DIABLO fused to GFP. When expressed in either 293T cells or NT2 cells, a punctate pattern of expression was observed indicating mitochondrial localization (Figure 6C).

DIABLO Is Able to Inhibit Protection of Cells by MIHA

To determine whether DIABLO was able to influence the antiapoptotic activity of MIHA, we chose a system in which expression of MIHA is critical for cell survival. Parental NT2 cells undergo apoptosis when exposed to UV radiation, but clones that stably express either Bcl-2 or MIHA do not (Figure 7A). We transfected these cells with vectors encoding DIABLO and GFP and analyzed those that had taken up the DNA, and hence were green, by flow cytometry and fluorescence microscopy. When exposed to UV radiation, cells stably expressing MIHA that were transfected with pEFLacZ remained highly viable, whereas the DIABLO-transfected cells were killed (Figure 7B, right panels, 7C filled bars labeled "MIHA-NT2 DIABLO," 7E). Sensitivity to UV radiation was not caused by transfection per se, because cells successfully transfected with a LacZ expression vector and the GFP construct rather than DIABLO and the GFP construct remained viable (Figures 7B, lower panels, and 7E). Transfection of DIABLO did not cause apoptosis in NT2 cells stably expressing MIHA (7B upper left panel, 7E) or Bcl-2 (Figure 7C empty bars labeled "Bcl-2 NT2"), in the absence of UV radiation. Like MIHA, Bcl-2 is able to protect NT2 cells from apoptosis induced by UV radiation (Figure 7A). However, DIABLO was not able to counter the protection against apoptosis afforded by Bcl-2 (Figure 7C). Transfection of wild-type NT2 cells with varying amounts of plasmids encoding MIHA and DIABLO showed that the ratio of IAP to DIABLO could determine whether a cell underwent apoptosis in response to a given dose of UV radiation (Figure 7D).

Discussion

Proapoptotic *Drosophila* proteins Grim, Reaper, and HID appear to function by interacting with IAPs, disengaging them from caspases, and thereby allowing cell death to proceed (Wang et al., 1999). While Grim, Reaper, and

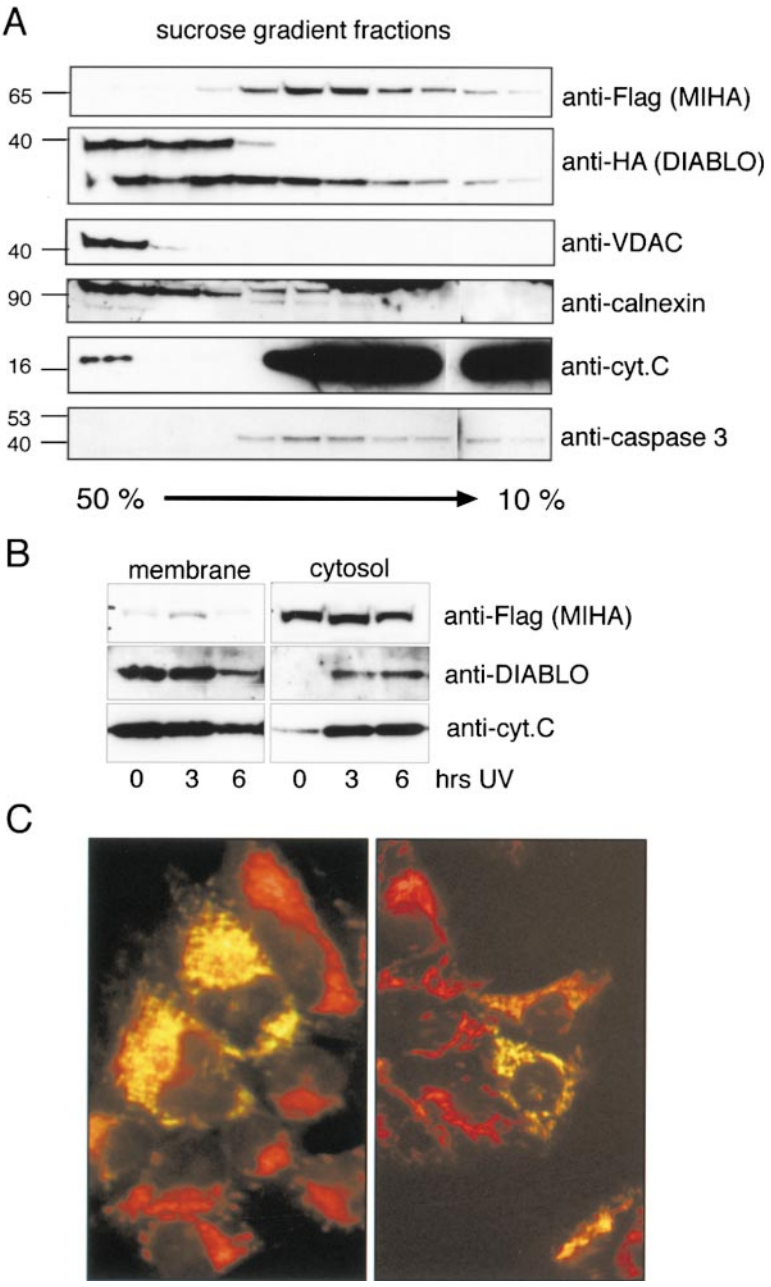

Figure 6. Subcellular Localization of DIABLO and MIHA

(A) Separation by sucrose gradient. 293T cells transiently transfected with Flag-MIHA and HA-DIABLO were lysed by passaging through a 27 G needle in a hypotonic buffer (see Experimental Procedures). The extract was then separated on a 50%–10% sucrose gradient and collected fractions examined for Flag-MIHA, HA-DIABLO, and a series of other proteins by Western blot analysis as indicated.

(B) Relocation of DIABLO from membranes to cytosol following UV irradiation. NT2 cells stably expressing Flag-MIHA were exposed to 50 J/M2 UV radiation and after the time indicated separated into membrane-associated and cytosolic fractions using Digitonin. An antibody kindly provided by Dr. Xiaodong Wang was used to reveal endogenous DIABLO.

(C) The amino terminus of DIABLO can target proteins to the mitochondria. The N-terminal 53 amino acids of DIABLO were fused to GFP, and the fusion protein was expressed in 293T cells (left) or NT2 cells (right). Cells were stained with mitotracker red and visualized by fluorescence microscopy. Yellow indicates colocalization of mitotracker red and GFP fluorescence.

HID are required for normal development in the fly, no mammalian homologs of these proteins have been identified (White et al., 1994; Grether et al., 1995; Chen et al., 1996). We describe here the identification of a novel protein DIABLO, which does not resemble any protein previously described but shares some functions with Grim, Reaper, and HID. Like them, DIABLO interacts with IAPs, including MIHA, MIHB, MIHC, and OpIAP, and interferes with the protective effect exerted by MIHA against UV radiation-induced cell death. Unlike Grim, Reaper, and HID, however, DIABLO does not appear to induce apoptosis in healthy cells and localizes to the mitochondria.

We initially observed human DIABLO as a 23 kDa protein with a low isoelectric point (pI = 5.3), which coimmunoprecipitated with MIHA. Full-length mouse DIABLO (29 kDa, pI = 6.1) undergoes N-terminal processing to yield the smaller form of the protein (23 kDa, pI = 5.4) that preferentially interacted with IAPs. The higher molecular weight form was restricted to membrane fractions, while the processed, IAP-interacting form was present in both membrane fractions and the cytosol where MIHA and caspase-3 were found. When we looked for endogenous DIABLO in healthy cells, we only detected the processed form, indicating that processing is not dependent on apoptosis. Endogenous DIABLO was concentrated in the membrane fractions of unirradiated NT2 cells but released following UV irradiation into the cytosol where it can interact with MIHA. Therefore, the proapoptotic activity of DIABLO appears

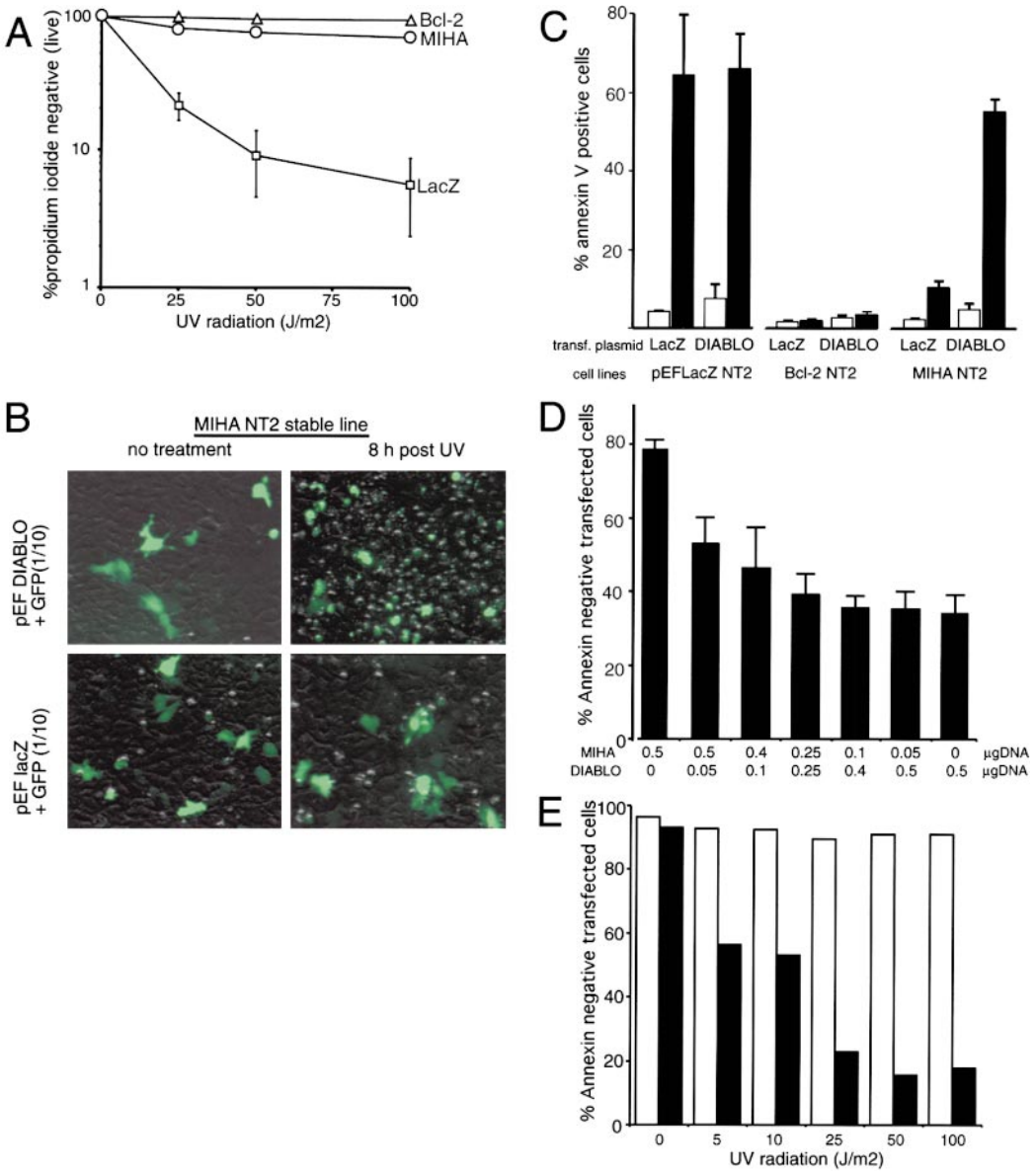

Figure 7. MIHA Protects NT2 Cells against UV Radiation and This Protection Is Antagonized by DIABLO

(A) NT2 cells stably expressing pEFLacZ, but not those stably expressing Bcl-2 or MIHA, undergo apoptosis when exposed to UV radiation. Cells were exposed to different doses of UV radiation and their viability determined by exclusion of propidium iodide (PI) 20 hr after exposure. Mean viability ± 2 SEM of three independent Bcl-2 clones, three independent MIHA clones, and four independent pEFLacZ NT2 clones are shown.

(B) NT2 cells stably expressing MIHA were transiently transfected with pEGFP and either pEFLacZ or pEFDIABLO expression constructs. After 48 hr, the cells were exposed to 25 J/M2 UV radiation and 8 hr later analyzed by microscopy (B) and flow cytometry (C). NT2 cells stably expressing MIHA, Bcl-2, or pEFLacZ were transiently transfected with either pEFLacZ or pEFDIABLO together with a GFP encoding vector. The percentage of GFP positive, annexin V positive (i.e., transfected, apoptotic cells) was determined by flow cytometry. Results represent the mean ± 2 SEM of three independent experiments for three independent MIHA lines, two Bcl-2 lines, and one pEFLacZ line.

(D) The ratio of DIABLO to MIHA can determine whether a cell undergoes apoptosis following UV irradiation. Wild-type NT2 cells were transfected with plasmids encoding GFP and MIHA and DIABLO in varying ratios and then exposed to 25J/m^2 UV radiation. The percentage of GFP positive, annexin V negative cells (i.e., live, transfected cells) was determined by flow cytometry. Error bars represent ± 2 SEM of three independent experiments.

(E) DIABLO interferes with MIHA-mediated protection from UV radiation-induced apoptosis over a wide range of UV doses. NT2 cells stably expressing MIHA were transfected with pEFLacZ (open bars) or DIABLO (filled bars) along with GFP and then exposed to UV radiation. The percentage of GFP positive, annexin V negative or positive cells (i.e., transfected, live or dead cells) was determined by flow cytometry.

to be controlled by its localization rather than by its processing. Because the amino terminal 53 amino acids of DIABLO were able to target GFP to the mitochondria and DIABLO associated with membrane fractions

DIABLO is likely to be a mitochondrial protein that is initially produced as a precursor protein that is proteolytically processed in the mitochondria to yield the smaller form. Processed DIABLO remains associated with the

membrane fractions in healthy cells, as does cytochrome c. Because following UV irradiation both proteins were simultaneously released from membrane fractions and accumulated in the cytosol, it is possible that the same mechanisms responsible for release of cytochrome c from the mitochondria are responsible for the translocation of DIABLO. Whereas cytochrome c could thereby interact with Apaf-1 (Zou et al., 1997), DIABLO would be able to interact with IAPs.

As well as being able to counter the protection afforded by MIHA against apoptosis caused by UV radiation in mammalian cells, DIABLO was able to reverse protection by MIHA against death due to expression of autoactivating caspase-3 in both *S. cerevisiae* and *S. pombe* model systems (data not shown). This is consistent with a model in which DIABLO directly interacts with IAPs to prevent them from inhibiting caspase activity and/or caspase activation.

DIABLO interacted with all the IAPs tested, including baculoviral OpIAP. While MIHA, MIHB, and MIHC have all been shown to bind to and directly inhibit caspases, direct inhibition of active caspases by OpIAP has not been described. For example, OpIAP protected insect cells from Reaper and UV-induced cell death but not from cell death induced by expression of active caspases (Seshagiri and Miller, 1997). The interaction of OpIAP with DIABLO presents an alternative route for OpIAP-mediated protection that does not involve direct caspase inhibition: OpIAP (and possibly other IAPs) may protect cells by sequestering cellular DIABLO, thus preventing it from disrupting the interaction of other IAPs with caspases. That DIABLO abrogated the protective effect exerted by MIHA against UV radiation-induced apoptosis but did not effect protection caused by Bcl-2 is consistent with Bcl-2 and MIHA regulating caspase activity independently.

Although DIABLO does not resemble Grim, Reaper, or HID, it is clear that the apoptosis pathways in insects and mammals are similar. In these organisms, the activity of caspases is regulated by IAPs as well as by adaptor molecules such as Apaf-1 or DARK. Just as these adaptors are subject to upstream control, for example by Bcl-2 family members, IAPs also appear to be regulated. DIABLO is the only mammalian protein to be identified that directly inhibits IAP function.

Experimental Procedures

Transfections and Constructs

The human embryonic kidney carcinoma cell line 293T was grown in RPMI media supplemented with 10% FCS, 1% penicillin-streptomycin, and 2% glutamine, and was transiently transfected with different mammalian expression constructs using polyethyleneimine as described. (Boussif et al., 1995). pEF BOS expression constructs encoding C- and N-terminally Flag-epitope-tagged MIHA (Flag-MIHA), C-terminally Flag-tagged MIHB (Flag-MIHB) and MIHC (Flag-MIHC), N-terminally Flag-tagged OpIAP (Flag-OpIAP), and N-terminally Flag-tagged CrmADQMD variant (Flag-DQMD) have been previously described (Uren et al., 1996; Ekert et al., 1999). A pcDNA3 vector (kindly provided by David Huang) construct encoding DIABLO with a Kozak initiation site and a C-terminal HA epitope tag was generated by PCR from IMAGE consortium clone 775927 (accession number AA276162) (HA-DIABLO). A pEF BOS expression construct encoding untagged DIABLO (Unt-DIABLO) with a Kozak initiation site was also generated. An expression construct encoding the N-terminal 53 amino acids of DIABLO fused to GFP within the vector pEGFP was similarly generated by PCR. The pcDNA3 expression constructs encoding unrelated HA-tagged proteins FLN29 (HA-FLN29) and ZAP1 (HA-ZAP1) were kindly provided by Jun-ichi Nezu and Shingo Toji, respectively. Transfection efficiency was visualized by cotransfection with a pEF BOS expression vector encoding green fluorescent protein. One to two days post transfection, cells were metabolically labeled with ^{35}S methionine in RPMI/10% FCS for a further 24 hr prior to lysis. Where indicated, cells were stained with mitotracker red (Molecular Probes).

The neuronal cell line NT2 was grown in DMEM supplemented with 10% FCS, 1% penicillin-streptomycin, and 2% glutamine. Stable NT2 lines were made using 1×10^7 NT2 cells transfected with 10 μg plasmid linearized with FspI and using lipofectamine (GibcoBRL). Forty-eight hours after transfection, cells were split into four separate plates and selected with puromycin (Sigma) 8 μg/ml. Puromycin-resistant colonies were selected, and expression of the transgene was determined by flow cytometry using anti-Flag M2 antibody (Sigma) or anti-Bcl-2 antibody (DAKO-Bcl-2 124) as previously described (Ekert et al., 1999). Transient transfection of NT2 cells was done using 20 μl Effectene (QIAGEN) and 4 μg of plasmid in 100 mm plates.

Cell Death Assays

Loss of cell viability was determined using propidium iodide (PI) uptake or annexin V staining assessed by flow cytometry (Becton Dickinson). For PI staining, cells were harvested from the plate with trypsin, centrifuged at 1500 rpm, and resuspended in PBS supplemented with 2% FCS and PI (1 μg/ml) (Sigma). For annexin V staining, harvested cells were incubated with biotinylated annexin V (kindly provided by Andreas Strasser) followed by incubation with Streptavidin-P. E. GFP positive cells were analyzed by flow cytometry for annexin V staining. Microscopy was performed on an Olympus microscope equipped with Hoffman and fluorescence optics.

Immunoprecipitations and Western Blot Analysis

Cells were lysed in a Triton X-100 based lysis buffer (10% Triton X-100, 10% glycerol, 150 mM NaCl, 20 mM Tris [pH 7.5], 2 mM EDTA, 1 mM PMSF, 10 μg/ml aprotinin, and 10 μg/ml leupeptin) for 1 hr, and the nuclear and cellular debris cleared by centrifugation. Immunoprecipitations were performed using Flag-specific mAb M2 covalently coupled to agarose beads (Sigma, Australia) and anti-HA antibody HA.11 (BABCO, Mannheim, Germany) plus protein G sepharose. The immunoprecipitates were washed five times in lysis buffer and proteins eluted with 100 mM glycine (pH 3). Proteins were separated by SDS PAGE or two-dimensional immobilized-pH-gradient (IPG)/SDS-PAGE (Pharmacia, UK) as described (Ji et al., 1997). Immunoprecipitates were examined by Western blot analysis or autoradiography following transfer of proteins to nitrocellulose membranes (Hybond C-Extra, Amersham, UK). mAbs used for Western blots were anti-Flag M2 (Sigma), anti-HA High Affinity 3F10 (Boehringer Mannheim, Mannheim, Germany), anti-cIAP1 (R&D Systems), anti-cIAP2 (R&D Systems), anti-cytochrome c (7H8.2C12, Pharmingen, USA), anti-VDAC (31HL, Calbiochem), anti-calnexin (N-terminal specific, Stressgen, Canada), and anti-caspase-3 (Pharmingen). Proteins were visualized by ECL (Amersham, UK) following incubation of membranes with HRP-coupled secondary antibodies.

Sucrose Gradient Fractionation

293T cells were transiently transfected with Flag-MIHA and HA-DIABLO. Forty-eight hours posttransfection, the cells were washed twice in PBS and lysed on ice in a hypotonic buffer (20 mM HEPES [pH 7.4], 5 mM $MgCl_2$, 10 mM KCl, 1 mM EDTA, 1 mM EGTA, 10 mM Tris [pH 7.4], 1 mM PMSF, 10 μg/ml aprotinin, and 10 μg/ml leupeptin) for 20 min followed by passaging 25 times through a 27G needle. Unlysed cells and debris were removed by centrifugation at 250 g for 5 min. The extract was then centrifuged over a 50%–10% sucrose gradient (in 20 mM HEPES [pH 7.4], 5 mM $MgCl_2$, 10 mM KCl, 1 mM EDTA, and 1 mM EGTA) at 40,000 rpm for 20 hr at 4°C in a Sw40 Ti rotor. Fractions were collected by puncturing the bottom of the tube and were analyzed by Western blot with various antibodies.

Protein Analysis and Mass Spectrometry

Proteins were separated by 2D immobilized-pH-gradient (IPG)/SDS-PAGE as described (Ji et al., 1997) and detected by staining of the

gel with Coomassie Phast-gel Blue R (Pharmacia, UK). Protein spots of interest were excised, digested in situ with trypsin (Moritz et al., 1996), resolved by capillary column reversed-phase HPLC (Moritz and Simpson, 1992), and identified by collision-induced dissociation (CID) tandem mass spectrometry (MS/MS) using a quadrupole ion-trap mass spectrometer (Finnigan model LCQ) equipped with electrospray-ionization (ESI) (Reid et al., 1998). Peptide amino acid sequences were determined by manual de novo interpretation of their b- and y-type production series (Roepstorff and Fohlman, 1984).

Northern Blot Analysis

Tissue-specific expression of DIABLO was examined by hybridization of a mouse tissue-specific Northern blot of poly A^+ RNA (Clontech) with a 720 bp ^{32}P-labeled partial cDNA probe encompassing the entire coding region for DIABLO. Equal RNA loading was confirmed by subsequent probing of the membrane with a β-Actin cDNA probe (Clontech).

Acknowledgments

This paper is dedicated to the memory of Lois K. Miller. We acknowledge Chris Hawkins, Gottfried Schatz, and Trevor Lithgow for their helpful suggestions, George Hausmann for technical advice, Peter Lock for coining the term DIABLO, David Huang and Andreas Strasser for biotin-annexin V, and Jun-ichi Nezu and Shingo Toji for plasmids. We particularly wish to thank the Wang lab for sharing information prior to publication and for kind provision of the antibody to Smac/DIABLO. This work was supported by an NHMRC grant to the WEHI (RegKey 973002). D. L. V. is a scholar of the Leukemia and Lymphoma Society. A. V. is a recipient of an NH and MRC CJ Martin Fellowship. P. E. is supported by a postdoctoral fellowship from the Royal Children's Hospital Research Institute. J. H. S. is funded by the Swiss National Fond.

Received November 22, 1999; revised May 18, 2000.

References

Alnemri, E.S., Livingston, D.J., Nicholson, D.W., Salvesen, G., Thornberry, N.A., Wong, W.W., and Yuan, J. (1996). Human ICE/CED-3 protease nomenclature. Cell *87*, 171.

Boldin, M.P., Goncharov, T.M., Goltsev, Y.V., and Wallach, D. (1996). Involvement of mach, a novel mort1/FADD-interacting protease, in Fas/APO-1- and TNF receptor-induced cell death. Cell *85*, 803–815.

Boussif, O., Lezoualch, F., Zanta, M.A., Mergny, M.D., Scherman, D., Demeneix, B., and Behr, J.P. (1995). A versatile vector for gene and oligonucleotide transfer into cells in culture and in vivo—polyethylenimine. Proc. Natl. Acad. Sci. USA *92*, 7297–7301.

Chen, P., Nordstrom, W., Gish, B., and Abrams, J.M. (1996). Grim, a novel cell death gene in drosophila. Genes Dev. *10*, 1773–1782.

Crook, N.E., Clem, R.J., and Miller, L.K. (1993). An apoptosis inhibiting baculovirus gene with a zinc finger like motif. J. Virol. *67*, 2168–2174.

Deveraux, Q.L., Takahashi, R., Salvesen, G.S., and Reed, J.C. (1997). X-linked IAP is a direct inhibitor of cell-death proteases. Nature *388*, 300–304.

Deveraux, Q.L., Roy, N., Stennicke, H.R., Vanarsdale, T., Zhou, Q., Srinivasula, S.M., Alnemri, E.S., Salvesen, G.S., and Reed, J.C. (1998). IAPs block apoptotic events induced by caspase-8 and cytochrome c by direct inhibition of distinct caspases. EMBO J. *17*, 2215–2223.

Dorstyn, L., Colussi, P.A., Quinn, L.M., Richardson, H. and Kumar, S. (1999). DRONC, an ecdysone-inducible *Drosophila* caspase. Proc. Natl. Acad. Sci. USA *96*, 4307–4312.

Du, C., Fang, M., Li, Y., Li, L., and Wang, X. (2000). Smac, a mitochondrial protein that promotes cytochrome c-dependent caspase activation by eliminating IAP inhibition. Cell *102*, this issue, 33–42.

Duckett, C.S., Nava, V.E., Gedrich, R.W., Clem, R.J., Vandongen, J.L., Gilfillan, M.C., Shiels, H., Hardwick, J.M., and Thompson, C.B. (1996). A conserved family of cellular genes related to the baculovirus IAP gene and encoding apoptosis inhibitors. EMBO J. *15*, 2685–2694.

Ekert, P.G., Silke, J., and Vaux, D.L. (1999). Inhibition of apoptosis and clonogenic survival of cells expressing crmA variants: optimal caspase substrates are not necessarily optimal inhibitors. EMBO J. *18*, 330–338.

Grether, M.E., Abrams, J.M., Agapite, J., White, K., and Steller, H. (1995). The head involution defective gene of Drosophila melanogaster functions in programmed cell death. Genes Dev. *9*, 1694–1708.

Hawkins, C.J., Uren, A.G., Hacker, G., Medcalf, R.L., and Vaux, D.L. (1996). Inhibition of interleukin 1-beta-converting enzyme-mediated apoptosis of mammalian cells by baculovirus IAP. Proc. Natl. Acad. Sci. USA *93*, 13786–13790.

Hawkins, C.J., Wang, S.L., and Hay, B.A. (1999). A cloning method to identify caspases and their regulators in yeast: identification of *Drosophila* IAP1 as an inhibitor of the *Drosophila* caspase DCP-1. Proc. Natl. Acad. Sci. USA *96*, 2885–2890.

Hay, B.A., Wassarman, D.A., and Rubin, G.M. (1995). *Drosophila* homologs of baculovirus inhibitor of apoptosis proteins function to block cell death. Cell *83*, 1253–1262.

Hu, Y.M., Benedict, M.A., Wu, D.Y., Inohara, N., and Nunez, G. (1998). Bcl-x-l interacts with Apaf-1 and inhibits Apaf-1-dependent caspase-9 activation. Proc. Natl. Acad. Sci. USA *95*, 4386–4391.

Irmler, M., Thome, M., Hahne, M., Schneider, P., Hofmann, B., Steiner, V., Bodmer, J.L., Schroter, M., Burns, K., Mattmann, C., et al. (1997). Inhibition of death receptor signals by cellular FLIP. Nature *388*, 190–195.

Ji, H., Reid, G.E., Moritz, R.L., Eddes, J.S., Burgess, A.W., and Simpson, R.J. (1997). A two-dimensional gel database of human colon carcinoma proteins. Electrophoresis *18*, 605–613.

Kaiser, W.J., Vucic, D., and Miller, L.K. (1998). The *Drosophila* inhibitor of apoptosis D-IAP1 suppresses cell death induced by the caspase drICE. FEBS Lett. *440*, 243–248.

Liston, P., Roy, N., Tamai, K., Lefebvre, C., Baird, S., Chertonhorvat, G., Farahani, R., Mclean, M., Ikeda, J.E., Mackenzie, A., et al. (1996). Suppression of apoptosis in mammalian cells by NAIP and a related family of IAP genes. Nature *379*, 349–353.

Moriishi, K., Huang, D.C.S., Cory, S., and Adams, J.M. (1999). Bcl-2 family members do not inhibit apoptosis by binding the caspase activator Apaf-1. Proc. Natl. Acad. Sci. USA *96*, 9683–9688.

Moritz, R.L., and Simpson, R.J. (1992). Application of capillary reversed-phase high-performance liquid chromatography to high-sensitivity protein sequence analysis. J. Chromatogr. *599*, 119–130.

Moritz, R.L., Eddes, J.S., Reid, G.E., and Simpson, R.J. (1996). S-pyridylethylation of intact polacrylamide gels and in situ digestion of electrophoretically separated proteins: a rapid mass spectrometric method for identifying cysteine-containing peptides. Electrophoresis *17*, 907–917.

Muzio, M., Chinnaiyan, A.M., Kischkel, F.C., O'Rourke, K., Shevchenko, A., Ni, J., Scaffidi, C., Bretz, J.D., Zhang, M., Gentz, R., et al. (1996). FLICE, a novel FADD-homologous ICE/Ced-3-like protease, is recruited to the CD95 (Fas/APO-1) death-inducing signaling complex. Cell *85*, 817–827.

Pan, G.H., O'Rourke, K., and Dixit, V.M. (1998). Caspase-9, Bcl-x-l, and Apaf-1 form a ternary complex. J. Biol. Chem. *273*, 5841–5845.

Reid, G.E., Rasmussen, R.K., Dorow, D.S., and Simpson, R.J. (1998). Capillary column chromatography improves sample preparation for mass spectrometric analysis: complete characterisation of human α-enolase from two-dimensional gels following in situ proteolytic digestion. Electrophoresis *19*, 946–955.

Roepstorff, P., and Fohlman, J. (1984). Proposal for a common nomenclature for sequence ions in mass spectra of peptides. Biomed. Mass Spectrom. *11*, 601–602.

Rothe, M., Pan, M.G., Henzel, W.J., Ayres, T.M., and Goeddel, D.V. (1995). The TNFR2-TRAF signaling complex contains two novel proteins related to baculoviral-inhibitor of apoptosis proteins. Cell *83*, 1243–1252.

Seshagiri, S., and Miller, L.K. (1997). Baculovirus inhibitors of apoptosis (IAPs) block activation of sf-caspase-1. Proc. Natl. Acad. Sci. USA *94*, 13606–13611.

Uren, A.G., Pakusch, M., Hawkins, C.J., Puls, K.L., and Vaux, D.L. (1996). Cloning and expression of apoptosis inhibitory protein homologs that function to inhibit apoptosis and/or bind tumor necrosis

factor receptor-associated factors. Proc. Natl. Acad. Sci. USA *93*, 4974–4978.

Vaux, D.L., and Korsmeyer, S.J. (1999). Cell death in development. Cell *96*, 245–254.

Wang, S.L., Hawkins, C.J., Yoo, S.J., Muller, H.A.J., and Hay, B.A. (1999). The *Drosophila* caspase inhibitor DIAP1 is essential for cell survival and is negatively regulated by HID. Cell *98*, 453–463.

White, K., Grether, M.E., Abrams, J.M., Young, L., Farrell, K., and Steller, H. (1994). Genetic control of programmed cell death in Drosophila. Science *264*, 677–683.

Zou, H., Henzel, W.J., Liu, X.S., Lutschg, A., and Wang, X.D. (1997). Apaf-1, a human protein homologous to *C. elegans* Ced-4, participates in cytochrome c-dependent activation of caspase-3. Cell *90*, 405–413.

GenBank Accession Number

The GenBank accession number for the sequence reported in this paper is AF203914.